Voltage Stability Assessment in Radial Distribution Systems: Leveraging Artificial Neural Networks for High Penetration of Solar PV and EVs

Kavya Suresh* , Kanakasabapathy P** , Saikat Chakrabarti** , Sanjib Kumar Panda***

- * Department of Electrical and Electronics Engineering, Amrita School of Engineering, Amrita Vishwa Vidyapeetham, India
- ** Department of Electrical and Electronics Engineering, Amrita School of Engineering, Coimbatore, Amrita Vishwa Vidyapeetham, India
 - *** Department of Electrical Engineering, Indian Institute of Technology, Kanpur, India
 - **** Department of Electrical and Computer Engineering, National University of Singapore, Singapore (kavyasuresh@am.amrita.edu, p_kanakasabapathy@cb.amrita.edu, saikatc@iitk.ac.in, sanjib.kumar.panda@nus.edu.sg)

[‡]Corresponding Author: Kanakasabapathy P, Department of Electrical and Electronics Engineering, Amrita School of Engineering, Coimbatore, Amrita Vishwa Vidyapeetham, India.

Received: 03.07.2025 Accepted: 13.08.2025

Abstract- The growing penetration of electric vehicles (EVs) and solar photovoltaic (SPV) systems in radial distribution networks increases system flexibility, yet poses severe challenges to voltage stability. Conventional approaches like Continuation Power Flow (CPF) and Jacobian-based sensitivity analysis (JBSA) offer accurate evaluations, but tend to be overly slow because of resource consumption. This paper proposes a com-bination of a data-driven approach to automate the assessment of voltage stability with a neural network approach for faster evaluation using a set framework of benchmarking scenario parameters to test boundary conditions at different levels of EVs and SPV penetration focused around the core elements of thwarting the system behaviour changes. The methodology strongly focuses around three parameters—Voltage Stability Index (VSI), Loadability Margin (LAM), and Generation Admissibility Margin (GAM)—that outline the system's ability to withstand further injections of load and generation while keeping the voltage within acceptable limits for stability analysis. The ANN model is developed with the load flow datasets obtained from the IEEE 33-bus radial distribution system as the training set. Out of all the learning algorithms used, the best accuracy was obtained with the Levenberg-Marquardt algorithm. This study is novel in its combined assessment of voltage stability under simultaneous high penetrations of SPV and EVs, which have traditionally been studied separately. The proposed Feed-forward ANN model uniquely estimates Voltage Stability Index (VSI), Loadability Margin (LAM), and Generation Admissibility Margin (GAM) concurrently, enabling adaptive, real-time monitoring. Unlike prior methods, our approach integrates data-driven machine learning with power system analysis for efficient, accurate prediction, providing practical insights for distribution network operators managing renewable and EV integration. Compared to conventional methods CPF (20.34 minutes, 7.64 MB) and JBSA (2.86 minutes, 21.90 MB), the ANN requires only 0.6 seconds and 3.03 MB, demonstrating significant gains in speed and memory efficiency. Results show the proposed ANN-VSI method effectively forecasts voltage stability margins, offering a practical alternative to traditional methods for real-time stability assessment in active distribution systems with high renewable energy and electric vehicle integration.

Keywords Solar photovoltaic (SPV) penetration, electric vehicles (EVs), voltage stability, voltage stability index (VSI), loadability margin (LAM), generation admissibility margin (GAM).

1. Introduction

Every aspect and activity in a person's life relies heavily on electricity. Therefore, an electrical power system can be viewed as having four main constituents: generation, transmission, distribution, and utilization [1, 2]. The latter is the most important because it addresses the increasing electricity demand that must be satisfied by the distribution network. Within these configurations, radial, mesh, loop, and network designs are used to sort out distribution of power to the customers effectively [3]. However, customer-oriented utilities tend to focus on radial distributions owing to its

operational simplicity. Due to the factors like urbanization, heavy industrialization, and rapid growth in population, worldwide demand for power has increased significantly in recent years. This creates additional challenges for power systems, including voltage instability, which can lead to blackouts [1]. There has been improvement and shift to sustainable energy resources to meet constant energy demands. In India, as of 31st July 2024, the PLI scheme with an estimated investment of 19,500 crores has resulted in an installed capacity of renewable energy of 150.276 GW and 87.21 of it being solar photovoltaic sponsored under the Ministry of New and Renewable Energy.

The increasing integration of SPV systems and EVs significantly influences voltage profiles in radial distribution networks. SPV generation can cause voltage rise during peak solar irradiance periods due to surplus active power injection, potentially pushing voltages beyond acceptable limits [4]. Conversely, EV charging loads can create sharp voltage drops during high demand periods, as the increased reactive and active power consumption stresses the network [5]. The simultaneous presence of both SPV and EVs results in complex voltage fluctuations, challenging conventional voltage regulation methods and risking voltage instability.

While numerous studies have independently examined the effects of SPV or EV penetration on voltage stability, limited research has addressed their combined impacts comprehensively. Moreover, prior works often focus on traditional analysis methods, lacking adaptive or real-time assessment tools capable of managing dynamic voltage changes in highly variable systems. This research addresses these gaps by developing an Artificial Neural Network (ANN)-based approach for real-time voltage stability assessment that accounts for the simultaneous integration of SPV and EVs, improving decision-making for system operation and planning.

This paper's novelty lies in the comprehensive consideration of both SPV and EV impacts on voltage stability within radial distribution systems, which is relatively unexplored. Unlike earlier studies focusing on individual effects or offline assessments, we develop a machine learning-based framework—specifically, a Feed-forward Artificial Neural Network—that simultaneously estimates key stability parameters (VSI, LAM, GAM) in real time. This integrated approach enables improved voltage regulation and system planning under dynamic operating conditions, supporting higher penetration levels of renewable energy and EVs with enhanced reliability.

1.1. Review of Relevant Literature

The integration of Solar Photovoltaic (SPV) systems and Electric Vehicles (EVs) is likely to introduce higher levels of intermittency and uncertainty into both generation and load demand within the power grid. Many researchers have analyzed the impact of SPV systems and EV charging on the operations of the grid, but quite little work has been done on the combined effect of both on grid stability, energy economics, and power quality [6-8]. Also, most of the studies do not address the topic of voltage stability extensively in distribution networks with high SPV and EV penetrations.

During times of high solar irradiance, SPV systems tend to increase voltage due to excess generation [9-11], whereas EV charging tends to reduce voltage during periods of high demand. The combination of these effects may lead to enormous and rapid changes in voltage that can overtax traditional voltage regulating devices and result in voltage instability or total system failure [12-13].

Several methods are available for evaluating voltage stability, including P-V curves, Q-V curves, sensitivity analysis, modal analysis, continuation power flow, and voltage stability indices [14]. Among these, Voltage Stability Indices (VSI) have garnered increased attention for online voltage stability monitoring, as they provide a quantitative metric to assess proximity to voltage instability in real time. VSI offer a single numerical value that directly represents the system's stability margin, making it easier to understand and apply compared to P-V and Q-V curves, which require graphical interpretation. Unlike sensitivity analysis, which only shows the indirect impact of system parameters on stability, VSI quantify the true stability margin, offering more actionable insights.

Additionally, VSI are computationally efficient compared to continuation power flow analysis, as they avoid iterative calculations and resource-intensive simulations. This makes them particularly useful for rapid assessments and real-time monitoring [15]. VSI also aid in optimizing the placement of SPV systems and EV charging stations by providing crucial information on voltage stability margins, enabling well-informed decisions that enhance system performance. Therefore, this study employs the VSI to identify strong and weak buses in the distribution network, facilitating the optimal placement of SPV and EVs [16].

Recent research has begun to explore the integrated effects of SPV and EVs on distribution networks using both conventional and intelligent techniques. A study in [17] proposed a coordinated control scheme with distributed PV to improve voltage stability and loadability in a modified IEEE-9 bus system. Hybrid metaheuristic optimization was applied in [18] to minimize voltage deviation and unbalance in PV-fed EV charging stations using Fire Hawk and Whale PSO algorithms on the IEEE-123 bus system. Comprehensive reviews such as [19] have highlighted the growing adoption of machine learning and FACTS devices for real-time voltage stability enhancement in renewable-dominant networks. A novel chance-constrained PV hosting capacity framework under uncertainty using Gaussian Process and Logit learning was introduced in [20], showcasing improved voltage risk prediction on IEEE 33- and 123-bus systems. Additionally, community-level analysis in [21] revealed that EV charging strategies directly influence PV investments and voltage stability in low-voltage grids, further emphasizing the need for adaptive control methods in future planning.

In addition to voltage stability, maintaining loadability and generation admissibility is critical for ensuring the reliability and stability of distribution systems with significant SPV and EV penetration. The loadability margin (LAM) ensures that the system can handle increased demand from EV charging without the risk of overload or significant voltage drops [22]. Meanwhile, the generation admissibility margin

(GAM) ensures the system can accommodate the variable output from SPV without causing voltage surges or overloading network components. Effective management of these margins allows the system to absorb fluctuations in both solar generation and EV charging patterns, maintaining stable voltage levels and preventing operational disruptions. Achieving this balance is essential for supporting the growth of renewable energy and electric transportation, while ensuring reliable distribution network operation. The estimation of the LAM and the GAM using a machine learning approach in a radial distribution system is one of the fundamental ideas introduced in this study for the reliable and stable operation of distribution systems with significant SPV and EV penetration. Accurate assessment of these margins is essential for regulating voltage stability under fluctuating load and generation conditions.

The attempt made by machine learning techniques, especially artificial neural net-works (ANNs), to predict voltage stability under various system contingencies and normal steady-state conditions has not succeeded due to the heavy dependence of these attempts on the feature selection process. In a number of previous works, several ANNs have been designed and trained to compute line-based voltage stability indices and the results have been satisfactory. Goh et al. [23] showed the effectiveness of ANNs to predict many line voltage stability indices (like Lmn, FVSI, VCPI, LCPI, etc.) in IEEE 9 and 14-bus systems and shown that they could reliably predict critical lines that were likely to fail due to voltages collapsing. Sharma et al. [24] also analyzed the effectiveness of some models such as Feedforward Backpropagation, Layer Recurrent and RBFN in predicting FVSI under different levels of reactive loading and stated that RBFN was the best performer in terms of predicting accuracy.

In this study, the ANN was trained using the dataset obtained from carrying out power flow studies of the Distribution system model in different scenarios [25]. Active power demand, reactive power demand, voltage angle, voltage magnitude, generated active power, loadability factor, and generation factor were among the input variables that formed the training data for the ANN. This comprehensive approach to voltage stability assessment, combined with machine learning techniques, aims to improve decision-making in voltage management and enhance the reliability of distribution systems with high penetrations of SPV and EVs. Also, this study used the IEEE 33-bus radial distribution system as a benchmark for comparison analysis with the proposed VSI based ANN model, utilizing Predictor-Corrector Continuous Power Flow [26-27] and Jacobian-Based Sensitivity Analysis (JBSA) [28] as the primary analytical methodologies.

1.2. Predictor-Corrector Continuous Power Flow

The Predictor-Corrector Continuation Power Flow (CPF) method is widely used for assessing voltage stability as well as performing loadability studies in power systems [29]. The method introduces a continuation parameter called λ which allows for systematic tracing of the power-voltage (P-V) curve in accordance with incremental loading or generation changes [22]. The CPF framework uses a two-phase procedure in which a predictor step first calculates the next solution point based on the current operating point using a tangent vector,

followed by a corrector step which applies Newton-Raphson iterations to improve the predicted solution. This method improves reliability of convergence in areas near the critical point of voltage collapse, where traditional power flow techniques often have difficulties achieving convergence. The predictor step computes the next state $(\hat{x}_{j+1}, \hat{\lambda}_{j+1})$ based on the previous point (x_j, λ_j) , a normalized tangent vector \overline{z}_j , and a predefined step size σ_j . The estimate is expressed as:

$$\begin{bmatrix} \hat{x}_{j+1} \\ \hat{\lambda}_{j+1} \end{bmatrix} = \begin{bmatrix} x_j \\ \lambda_j \end{bmatrix} + \sigma_j \,\bar{z}_j \tag{1}$$

Subsequently, the corrector step ensures that the solution satisfies both the power flow equations $f(x, \lambda) = 0$ and a parameterization constraint. This paper employs a pseudo arclength formulation to ensure numerical continuity across turning points defined by [24]:

$$\phi_{j}(x,\lambda) = \begin{bmatrix} x - x_{j} \\ \lambda - \lambda_{\lambda} \end{bmatrix}^{T} \bar{z}_{j} - \sigma_{j} = 0$$
 (2)

However, a notable disadvantage of this method would be the heavy computational time, especially when it comes to larger systems demanding many continuation steps and corrections.

1.3. Jacobian-Based Sensitivity Analysis (JBSA)

The JBSA approach provides an analysis technique using the Jacobian matrix obtained from the power flow equations' linearized set to study the impact of active and reactive power injections on the voltage level at the buses, assuming the bus voltage magnitudes operate within a specific value. This approach stems from the Newton Raphson method where the nonlinear power flow equations are solved using first-order Taylor series expansion about an operating point. Such approach defines the Jacobian matrix J, which is composed of partial derivatives of power injections with respect to voltage magnitudes and angles, as a basis for sensitivity calculation. Quantitative sensitivity computation comes of matrix inversion that expresses small perturbations on power as [28]:

$$\begin{bmatrix} \Delta \delta \\ \Delta \nu \end{bmatrix} = J^{-1} \begin{bmatrix} \Delta P \\ \Delta Q \end{bmatrix}$$

where ΔP and ΔQ are incremental changes in real and reactive power, and $\Delta \delta$ and ΔV are the corresponding variations in voltage angle and magnitude. Although JBSA provides an organized structure based on mathematics for performing voltage sensitivity analysis, it has considerable constraints concerning its usage in radial medium voltage distribution systems, and it also uses much more storage on computer memory.

1.4. Contribution and Paper Organization

Compared to the existing literature, this paper offers the following

➤ It analyzes the scope of the impact concerning the individual and synergistic effects the SPV and EVs have on voltage stabilization in a distribution system.

- ➤ It determines strong and weak buses in the distribution network with the help of VSI, thus facilitating appropriate location of SPV system and EV charging stations.
- ➤ It defines the limits within which the dual parameters LAM and GAM for selected buses are maintained to ensure system resiliency and reliable operation for different load and generation profiles.
- ➤ It constructs, trains, and validates a Feed-forward ANN model for VSI, LAM, and GAM estimation at the selected buses using various algorithms, thereby enabling real-time adaptive voltage stability monitoring and responsive intervention.
- ➤ It analyzes JBSA and the conventional method of Predictor-Corrector Continuous Power Flow against the proposed VSI-based ANN method, thus enhancing under-standing of the former's efficacy.

The rest of this paper is structured as follows: In Section 2, the fundamentals of volt- age stability are discussed, which includes the definitions and formulations of Voltage Stability Index (VSI) as well as LAM and GAM. In Section 3, I provide detailed explanation of the proposed ANN-based estimation technique of VSI, LAM, and GAM. The Section 4 offers commentary on the results obtained from the simulations and discusses them further. In the concluding section, provide definitive remarks while clarifying the principal findings of this study in Section 5.

2. Fundamentals and Definitions

The importance of maintaining an adequate voltage level in radial distribution systems is of core interest in dependable power delivery, more so in systems with a pronounced blend of renewable energy technologies and electric vehicles. Moreover, due to the simple and single-path nature of radial systems, which is easily subjected to changes in load and distributed generation, radial systems are more susceptible to voltage deviation. This part seeks to explain the most voltage stability aspects of radial networks along with the fundamental and important definitions in regard to voltage stability in such networks.

2.1. Voltage Stability

"Voltage stability" describes a power system's efficacy in maintaining the voltages at each bus within reasonable bounds nearby the nominal value, and also requires that no singularities arise from flexible disturbances [30]. It is fundamentally connected with how well the system can balance the supply and demand of the electric load.

Table 1. Comparison of VSI based on analytical approach

efficiency in the grid.

According to [14, 32], VSIs can be taught modulating like wigs in different photographs because of their methodologies and context of usage.

VSI based on Jacobian matrix's operations

VSI based on the system variables

VSI Global, Bus, Line and individual VSI

Voltage instability is often observed as slow decay or increment of the voltage level at some particular bus. The addition of SPV systems and EVs to distribution networks brings new challenges that can worsen voltage instability. Fluctuating solar power generation and the nonexecutable nature of load forecasting such as EV charging impose tremendous voltage deviation. The overvoltage phenomenon that may occur during peak solar irradiance periods is due to excess power produced when the local distribution network is poorly designed or equipped to control these fluctuations [31]. At the same time, these systems can be further exacerbated by additional EV demand during charging periods which stresses the infrastructure, resulting in further voltage depression or oscillation and system destabilization.

2.2. Voltage Stability Index (VSI)

The VSI metric is a quantitative measure used to gauge the voltage stability of power distribution networks. It enables the online operation of the system, indicating the stability margins and maximum loadability of the system's various elements. VSIs serve to determine possible weak areas, like transmission or distribution lines or buses, that need detailed compensation or reinforcement by evaluating these factors. VSIs can be assessed on different levels from single distribution lines, buses, or for the entire network, allowing for comprehensive evaluation of the stability analysis.

Using IEEE 14 bus model system of South Yorkshire, VSIs are calculated to pinpoint weak and strong voltage stability nodes in distribution system. This is highly useful in the case where DERs such as SPV systems are to be integrated optimally and when planning for grid EV charging stations. Through the distribution grid level set lower bounds for adjustable set points at weak buses to enhance voltage stability, reduce voltage collapse risk, and energy distribution efficiency in the grid.

Jacobian matrix-based VSI	System variables-based VSI
Suitable for offline applications	Suitable for online applications
Determine the voltage stability margin	Identify the weak busses or lines
Require more computational time	Require less computational time

Table 1 analyzes the classification and merits of different types of VSI. Although these methods are accurate, they are highly complex calculations and very sensitive to changes in topology, as changes to the network cause its formulae to recalculate its Jacobian matrix. This makes weakly monitoring voltages in real-time via a Jacobian — S-map order discrimination matrix approach impractical [33]. Also, with these methods, their longer calculation time increases the level problem of integrating distributed generation (DG).

However, system variables based models are better focused to real time purposes, since they have lower computation workload. These types of models fall short though because they overestimate the severity of voltage instability and thus fail to provide useful boundary information completeness of VSM assessment [34].

Table 2 presents the classification of VSI into three types along with their advantages and disadvantages: line-based, bus-based, and global indices. Each type of VSI has merits and demerits. The former analyzes the stability aspect of voltage through transmission lines, measuring the ability of each line to maintain voltage level under load growth. These indices enable grid operators to disable further load increases before critical in- stabilities occur on certain voltage levels. Busbased VSI measures the voltage stability of particular nodes or buses in the network and the level of each bus to collapse voltage [35]. Some important indices are VCPI [36] and Lindex [37], which analyses voltage instability from point of view of a bus at certain load and give information about those busses which are near minimum under voltage region with some sanity for grid system. Finally, global indices offer holistic assessment of voltage stability from the point of view of entire power system.

which include evaluation of flow of load in the network, to assess the overall stability of the system and the vulnerabilities on which inference can be drawn at higher level.

These indices utilize number of system-wide parameters

In order to facilitate the implementation of SPV and EVs, this research paper employs a bus VSI to identify weak and strong buses in the radial distribution system [16, 38, 39, 40]. Figure 1 illustrates a simplified two-bus equivalent distribution network that helps how VSI for a specific bus j, i.e. VSI_j is determined using Equation (3) given below [16].

$$VSI_{i} = V^{4}_{i} - 4(P_{i}R_{ij} + Q_{j}X_{ij})V_{i}^{2} - 4(P_{i}X_{ij} - Q_{i}R_{ij})^{2}$$
(3)

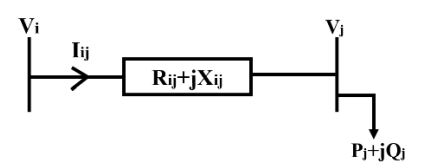


Fig. 1. Simplified distribution network.

Where, i and j are the sending and receiving buses; P_j and Q_j are total effective active and reactive power at the receiving bus; and R_{ij} and X_{ij} are the line resistance and reactance between the buses i and j respectively. In a distribution system, the Voltage Stability Index (VSI) varies between 0 and 1.

The system's ability to effectively maintain voltage levels under varying load conditions is indicated by a value of 1, whereas a value of 0 indicates a high susceptibility to voltage collapse and very low voltage stability.

Table 2. Comparison of VSI based on specific focus area

Type	Merits	Demerits
Line VSI	(i) Simple and easy to implement (ii) Identifying	(i) Lower accuracy (ii) Energy
	sensitive lines (iii) Appropriate techniques for	flow constraints limit the ability of most indices to
	determining the network's stability (iv) Reduced	predict system behavior beyond the collapse point
	computation time	
Bus VSI	(i) Useful for real-time ap-	(i) Implementation of these indexes are more
	plications (ii) Identifying sensitive buses (iii) Simple	challenging
	and easy to implement	
Global	(i) Better accuracy (ii) Better	(i) Has limitations when used
VSI	tool for predicting power system instability and	to radial systems (ii) Complexity in calculation
	transmission capability	

2.3. Formulation of Loadability Margin (LAM)

The LAM monitors the maximum additional load which the distribution network can stand without collapsing, particularly with respect to rising EV charging demands. The coming of EVs into the market brings about abrupt changes in grid demand, which if not properly controlled, can result in systems being overloaded, voltage drops, and or even system instability. To ensure these effects, to guarantee proper operation within the system while minimizing disruption, it is needed to preserve an adequate level of adaption management typically illustrated by a P-V curve.

For calculating LAM, this study computes in intervals the active and reactive power demand of specific buses in the distribution system. More specifically, the buses with the maximum VSI values are analyzed and determined to be the most durable. Strong buses with high initial VSI values comprise Buses 2, 3, 4, 20, 23, 26, 30, and they serve as the basis for EV load placement. As for EVs, they are represented as basic dynamic loads at the bus level which further increases the demand for active and reactive power in Grid- to-Vehicle (G2V) mode with a loading factor λ . As per equations (4) - (6), they will be gradually adjusted according to a predefined strategy [41].

This modeling reflects typical real-world usage, where the majority of EVs draw power from the grid without supplying it back. While vehicle-to-grid (V2G) operation enables EVs to act as distributed energy resources by injecting power into the grid during peak demand or voltage instability, V2G functionality is intentionally excluded from this work as the study simultaneously incorporates significant penetration of solar photovoltaic (SPV) generation, which introduces variability in voltage profiles and acts as a form of distributed generation. By limiting EVs to G2V mode, the study isolates the effects of EV charging demand on the distribution system's voltage stability and availability margins under fluctuating SPV conditions. This provides clearer insights into the challenges posed by increasing EV adoption when combined with intermittent renewable generation.

$$P_{dj,new} = P_{dj,old}(1 + \lambda) \tag{4}$$

$$Q_{dj,new} = Q_{dj,old}(1+\lambda) \tag{5}$$

$$\lambda = \lambda_{\text{old}} + \delta_{\text{d}} \tag{6}$$

In the previous iteration for bus j, real and reactive power demand are denoted as $P_{dj,\text{old}}$ and $Q_{dj,\text{old}}$, respectively. Also, for bus j, new adjusted values of increased loading factor λ are noted as $P_{dj,\text{new}}$ and $Q_{dj,\text{new}}$ with δ_d rate. Hence, the divergence of load flow is defined to capture the maximum loadability threshold. This process is repeated until the system arrives at its voltage stability point, thereby defining the upper LAM limit. The algorithm to compute the upper limit LAM for the chosen buses is displayed in Figure 2.

Figure 2 shows the LAM and GAM Margin estimation work flow employing the IEEE 33-bus radial distribution system. Initially, a base case study of load flow checking is carried out to determine voltage (V_i) at the bust's, power's elements (P_i, Q_i) and also line parameters (R_{ij}, X_{ij}) . As a result, The VSI (VSI_i) is computed for each bus. Then it branches into two portions, the weaker one corresponding to the bus with minimum VSI_j for generation increment (Pgj) estimate GAM, and to the strongest one corresponding to the bus with maximum VSI_i for load increment (P_dj, Q_dj) and estimate LAM. This step is practically executed by successively adjusting the generation or load, performing load flow analysis in each step while updating the VSI until Voltage or Vice state indicator constraints are breached. Under those conditions, the final outputs for λ and ϵ values are retrieved as maximum LAM and minimum GAM values correspondingly. The method provides voltage stability limits of the tested buses when subjected to increasing loading or generation increments.

In the described approach, VSI_{jmin} and VSI_{jmax} denote the minimum and maximum bounds of the VSI (Voltage Stability Index) value measures across all buses in the base case load flow which is the basic range for controlling generation and load stepping loops to maintain stability with designated values $0 < VSI_j < 1$ and $0.95 \leq V_i \leq 1.05$.

2.4. Formulation of Generation Admissibility Margin (GAM)

It is crucial to estimate the GAM to manage the variability of SPV generation. The supply demand equilibrium is affected by the intermittent power generation caused by SPV systems.

The GAM marks the boundary of generation increase which does not destabilize the system. The distribution system can maintain stability and cope with the oscillations created by the penetration of solar power if this margin is preserved. The real power at the selected buses with lower VSI values in the distribution system is gradually increased by a generator factor ϵ defined in Equations (8)-(9) for the purposes of calculating GAM. Buses such as 7, 8, 16, 19, 24, 32, and 33 with low VSI values are identified for optimal selection for SPV integration, considering them as simple generators to evaluate power system voltage stability for stressed case scenarios assuming the bus is a PQ type and converted to PV type once $P_{\rm G} > P_{\rm D}$ while power at the bus is determined using the equation,

$$P_{\text{net}} = P_{\text{dj,gen}} - P_{\text{gj,new}} \tag{7}$$

$$P_{gi,new} = P_{gi,old}(1 + \epsilon)$$
 (8)

$$\epsilon = \epsilon_{\text{old}} + \delta_{\text{g}}$$
(9)

Here $P_{gj,old}$ means the real power that was injected earlier, and $P_{gj,new}$ are the new updated power values after a generation change ε is applied at rate $\delta_g.$ The algorithms for estimating the maximum GAM for the selected buses is also explained in Figure 2.

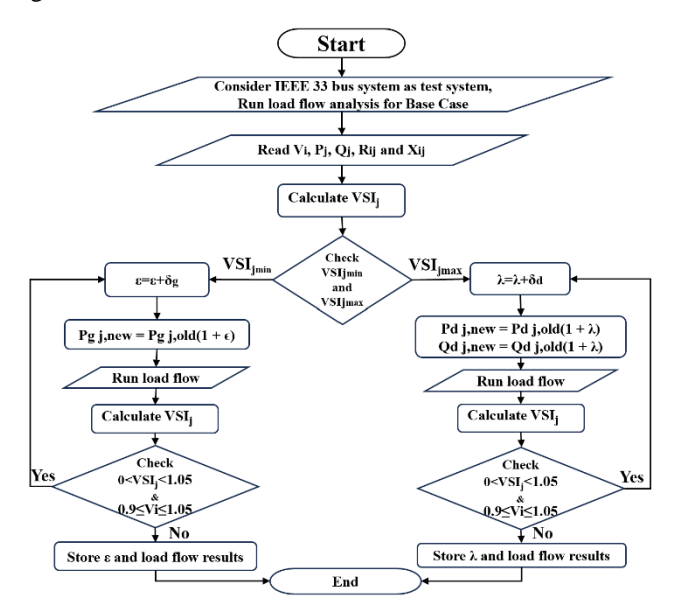


Fig. 2. Flowchart for estimation of maximum loadability margin (LAM) and generation admissibility margin (GAM).

3. Methodology of the Proposed Artificial Neural Network Based Estimation of VSI, LAM and GAM

The VSI in this context refers to system's ability to maintain the definition of stable system voltage under fluctuations from renewables or EV loads. LAM is how much more extra load is added to the system to make it unstable, and generation margin is the system capability to service load compared to available generating resources. With the help of estimating VSI at a bus, combining with LAM and GAM using ANN, it is possible to integrate the SPV and EVs reliably to the radial distribution system. ANNs plays significant roles in estimating and maintaining voltage stability.

Prior works, including in [22], suggested the application of various machine learning techniques like artificial neural networks (ANNs) and support vector machines (SVMs) for forecasting LAMs or voltage stability. This work employed a machine learning approach with a Feed Forward ANN model to predict VSI and availability margins in distribution systems with high SPV and EV penetration. Figure 3 illustrates the ANN-based method diagram for evaluating stability in a radial distribution system 3.

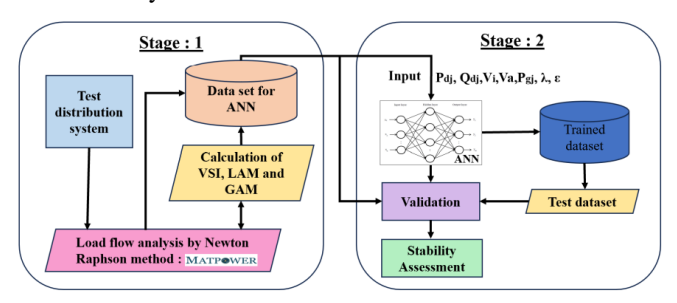


Fig. 3. Proposed ANN-based system for stability assessment.

3.1. IEEE 33 Bus Test System

The IEEE 33-bus radial distribution system is used as a test bed in this study to enable the examination of voltage stability assessment, as illustrated in figure 4. An example of a medium-voltage distribution network is the IEEE 33-bus system, which consists of 33 buses and 32 branches and operates at a nominal voltage of 12.66 kV [42]. This test system is well known for assessing how distributed energy supplies affect stability margins and voltage profiles [43]. As shown in figure 4, the particular buses assigned to SPV integration and EV charging station penetration are identified. The dynamism and complexity of the system are increased when EVs and SPV systems are integrated. Significant SPV integration influences voltage profiles and power flow because to its variability, whereas EVs provide extra load, potentially resulting in under voltage circumstances. The integration of SPV and EV proliferation in the system intensifies voltage stability issues.

Solar Photovoltaic (SPV) systems are considered as distributed generators (DGs) placed at respective buses and are treated as conventional generation sources; in case their active power flows (output) is more than the local demand (P_G $> P_D$), the corresponding bus will switch from PQ to PV mode to enable voltage control operation. In this configuration, electric vehicles (EVs) are modeled as dynamic secondary loads that increase both active power and reactive power at particular buses in Grid-to-Vehicle (G2V) mode. This provides the fluctuation potential of renewable generation together with the variability of load due to EVs. This paper's load modeling takes into consideration both the base loads of the IEEE 33-bus network as well as the additional ones resulting from EV integration at certain buses. In selected buses, EV loads are added incrementally while the original residential and commercial loads at all other buses are kept. This guarantees that the existing network demand along with the new EV loads is accurately captured, providing analysis into the depth of voltage stability and system interactions.

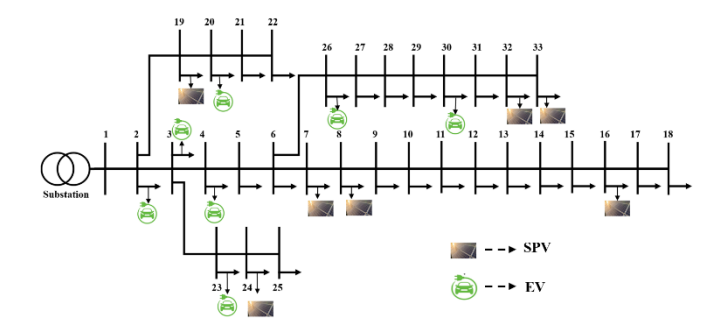


Fig. 4.Schematic of IEEE 33 bus radial distribution system with EV and SPV penetration.

To obtain the necessary initial datasets for ANN training, load flow solutions of the IEEE 33-bus radial distribution system with varying penetration levels of SPV and EVs are considered. Data required for the calculation of VSI are obtained through load flow analysis of the distribution system using the MATPOWER. After determining the VSI for the base case, buses with low VSI values are identified for SPV installation, while buses with higher VSI values are designated for EV charging infrastructure.

3.2. Architecture and Training of the ANN

ANN can learn complex non-linear input-output relationships through training without the need for explicit programming. Due to this learning ability, they perform effectively even in untrained scenarios. This study utilizes ANN's capability to estimate the VSI and availability margins in distribution systems under high SPV and EV penetration.

The efficiency of a neural network is critically dependent on the selection of input variables. The input variables selected for this research include active power demand (P_{di}) , reactive power demand (Q_{di}) , bus voltage magnitude (V_i) , voltage angle (Θ_i) , real power injected (P_{gi}) by SPV, loadability factor (λ) , and generation admissibility factor (ϵ) . In this work, the choice of input variables is based on their impact on voltage stability as well as alignment with the Jacobian-Based Sensitivity Analysis (JBSA) benchmark. A JBSA's primary function is to assess the measure of sensitivity of a system's voltage to a set of controllable parameters designated as: as (P_{di}) , (Q_{di}) , and (P_{gi}) . Likewise, state variables V_i and Θ_i represent power flow analysis and form a basic kernel needed to describe the system behavior over a range of operating conditions. Moreover, λ and ϵ serve as high level voltage instability indicators. This unique blend guarantees that the ANN captures stability margins at nodal level and system level, making possible the use of more common analytic approaches. Taking into account the selected input variables from the 33 buses, the input pattern for the neural network consists of 7 arrays of 33 variables, each as input. VSI, LAM, and GAM are selected as output variables for the ANN to evaluate voltage stability in a radial distribution system with high penetration of SPV and EV, so the output pattern for the neural network consists of three arrays of 33 variables each as output. The model can efficiently assess and track voltage stability by training the ANN to anticipate these output variables. This enables proactive management and optimization of the distribution network in various scenarios of integrated energy and electric vehicle charging stations.

Artificial neural networks (ANNs) predict these output variables. Thus, the model efficiently analyzes and regulates voltage stability. This simplifies proactive monitoring and updating of distribution networks in scenarios with the integration of electric vehicle charging stations and distributed energy. Electric vehicles and distributed energy are integrated in these situations. Thus, a distribution system with 33 buses will have three arrays with 33 variables each as its output pattern.

An artificial neural network with a single hidden layer made up of ten neurons was determined to be the best architecture for the suggested system after iterative testing. The ANN architecture is shown in Figure 5. The ability of a feed-forward artificial neural network to incorporate nonlinearity and recognize complex patterns is evaluated using nine different activation function combinations. Because they can efficiently link input to output without the complications that come with recurrent architectures, feed-forward artificial neural networks are preferred. For comparative analysis, four training algorithms are also used: Resilient Propagation, Scaled Conjugate Gradient, Gradient Descent with Momentum, and Levenberg-Marquardt.

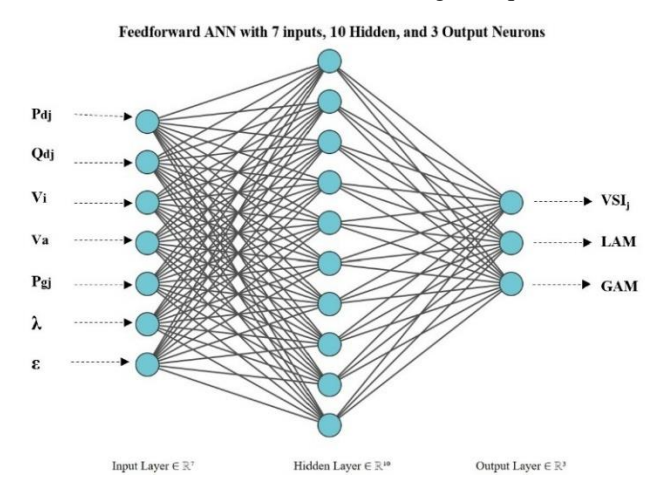


Fig. 5. Architecture of ANN.

3.3. Identification of Possible Scenarios and Generation of Data Set for Training and Validation of ANN

The identification of potential scenarios and generation data sets for voltage stability assessment and prediction of availability margins in the IEEE 33 radial test distribution system requires investigation of various penetration levels of SPV and EV. Scenarios for SPV penetration need to take into account how the variable nature of solar generation affects voltage stability and the system's capacity to accommodate additional generation demand, i.e., GAM. When it comes to EV penetration, the emphasis switches to how more charging loads impact LAM, along with any possible voltage drop issues during peak charging periods.

When both SPV and electric vehicles are present, scenarios must account for the dual effects of increased demand from electric vehicles and variable output of the SPV. This combined analysis helps predict the voltage stability of the system under varying demand patterns and fluctuating generation conditions. It also helps to evaluate the GAM by figuring out how much additional generation can be added to

the system while maintaining voltage stability, as well as LAM by determining the maximum load the system can handle before voltage problems occur.

Conventional power flow analysis is employed to generate datasets across various EV and SPV penetration scenarios. The first step is the calculation of the VSI for the base case scenario in the IEEE 33-bus radial distribution system to identify buses with lower VSI values. The identified buses are subsequently supplemented with SPV generation, which is gradually increased until the bus voltage magnitude (V_i) remains within the safe range of 0.9 to 1.05 per unit and the VSI is maintained between 0 and 1 to ensure stable operation. When the generation surpasses the load demand at a specific bus, the bus is converted into a PV bus, which signifies its new function in promoting voltage stability and improving the overall reliability of the system. In this research work a total of 116 scenarios are generated for various levels of SPV penetration case. The SPV generation at the specific buses was incremented by 10% units of the local load until the generation surpassed the demand $(P_G > P_D)$, as well as voltage magnitudes and VSI (0.90 p.u \leq V_i \leq 1.05 p.u, 0 < VSI < 1) reached their limits.

The second case of the analysis, EV charging is treated as an extra load in the IEEE 33 distribution system. This load is applied to the buses with higher VSI values in the base case scenario. The load is increased until the bus voltage magnitude (Θ_i) and VSI remains within the specified limits to maintain voltage stability. The impact of this load increase is penetration extensively investigated by generating a total of

428 scenarios, which enables a detailed evaluation of the impact of varying levels of EV charging on system performance and stability under these constraints. In the same manner, EV loads were added at the selected buses in 10% steps of the base load until the VSI becomes 0, indicating the stability boundary, and bus voltages remained within acceptable limits.

In the third case, both SPV and EV charging stations are considered simultaneously. In order to conduct a comprehensive analysis of the effects, 658 different scenarios were created. SPV systems and EVs are integrated simultaneously at identified buses into the IEEE 33 radial distribution system to examine the combined impacts on voltage stability. To evaluate the effect on the voltage profile of the system, this scenario included gradually increasing the penetration levels of SPVs and EVs. The analysis was specifically designed to ensure that the VSI and voltage magnitudes (Vi) remained within predetermined limits as the penetration levels of SPV and EV were increased. This was done in order to assess the impact of integrating EVs and SPVs at the same time on voltage stability and to determine the maximum penetration levels that the system is capable of handling without affecting stability.

Table 3 gives the detailed summary of scenarios generated for the three different cases. The dataset is divided into 70% for training, 15% for validation, and 15% for testing in each of the categories, with 841 training samples, 180 validation samples, and 181 testing samples from a total data set of 1202.

Table 3. Various possible scenarios of SPV and EV

Sl. No	Load Bus	Generation Bus	No. of Scenarios
•		Base Case	
1			1
		With SPV Penetration	
2		7	12
3		8	12
4		16	22
5		19	22
6		24	13
7		32	13
8		33	22
l .	W	ith EV Charging Station	ı
9	2		38
10	3		61
11	4		33
12	20		47
13	23		130
14	26		104
16	30		14
	With S	PV and EV Charging Station	
16	2	7	39
17	3	8	63
18	4	16	39
19	20	19	57
20	23	24	109
21	26	32	121
22	30	33	11
23	3, 20	24, 32	46
24	2, 3, 4,	16, 24, 33	39
25	2, 4, 20, 26,	8, 16, 32, 33	39
26	4, 20, 23, 26, 30	7, 8	22
27	3, 4	16, 19, 24, 32, 33	45
28	2, 3, 4, 20, 23, 26, 30	7, 8, 16, 19 24, 32, 33	28
Total			1202

3.4. Computational Efficiency and Model Complexity

The computational efficiency of the ANN-based voltage stability estimator depends on both the ANN architecture and the complexity of the distribution network model used for training and inference.

From the ANN model perspective, the current feedforward network size was selected to strike a balance between predictive accuracy and resource usage. While reducing the number of neurons or layers can decrease prediction time and memory footprint, preliminary experiments showed that smaller networks compromised the accuracy of Voltage Stability Index (VSI), Loadability Margin (LAM), and Generation Admissibility Margin (GAM) predictions. Thus, the current ANN architecture provides reliable results within a reasonable computation time and memory usage.

From the distribution network perspective, reducing the network size (e.g., simplified models with fewer buses or aggregated loads) would reduce the dimensionality of ANN inputs, leading to smaller networks and faster computation.

However, such simplification may limit the model's applicability and accuracy in representing voltage stability issues at a detailed level, especially in radial distribution systems with high penetration of solar photovoltaic (SPV) and electric vehicles (EVs) on each and every busses. Maintaining a sufficiently detailed network model is essential to capture spatial variability in voltage profiles and stability margins accurately.

It is important to note that the present study employs an offline, background evaluation approach, wherein the ANN is trained and validated using extensive simulated datasets generated from power flow analyses under various system conditions. This offline training framework allows for the use of more complex models without the computational constraints inherent in real-time processing. Once trained, the ANN model can be deployed for near real-time voltage stability monitoring and decision-making of the system with considerable change in system conditions, where the achieved prediction latency of fraction of second is acceptable for operational use. The system used to run the ANN-based model features an 11th Gen Intel Core i7-11370H processor with a base clock speed of 3.30 GHz and 16 GB of RAM, which provides sufficient computational power and memory bandwidth for fast execution of lightweight neural networks. Its strong single-core performance facilitates rapid inference even without dedicated hardware accelerators, which justifies the model's quick prediction time and minimal memory consumption.

3.5. Generalizability and Applicability to Real-World Distribution Networks

Though the proposed ANN model is developed and validated on the IEEE 33-bus radial distribution system, it ensures generalizability towards any real-world distribution network through multiple design considerations as follows:

- ➤ It is trained on a wide range of operating conditions (varying load, SPV, and EV penetration) to capture general voltage stability behaviours beyond a single network.
- ➤ Input features—active/reactive power, voltages, loadability, and generation factors—are fundamental electrical parameters common across most radial distribution networks.
- The ANN architecture is adaptable and can be finetuned and retrained with any real-time distribution system data to accommodate different network sizes and topologies.
- The ANN framework supports retraining with suitable input output vectors with realistic data of any target practical distribution network, enabling the model to incorporate system-specific characteristics.

Hence, this comprehensive approach ensures that the proposed ANN model maintains accuracy and reliability when applied beyond the benchmark IEEE 33-bus system, validating the model on larger, real-world distribution systems to confirm scalability and robustness.

4. Simulation Results and Discussion

The proposed methodology is simulated in IEEE 33-bus radial distribution system as a test bed using MATLAB. The ANN, as described in Section 3.2, is employed to estimate the VSI, LAM, and GAM for the selected test system. The dataset generated, as described in Section 3.3, is used for training, testing, and validating the proposed voltage stability assessment.

4.1. Performance of the Trained ANN

Every input pattern for the ANN consists of 231 inputs from the IEEE 33 distribution system and, as outlined in Section 3.2, the output pattern contains 99 outputs. After a number of cycles in testing, the chosen architecture in their ANN, which used the tan-linear activation function with the Levenberg-Marquardt training algorithm, demonstrated optimum results. This architecture had 10 neurons in the hidden layer, as shown in Figure 6, which is discussed below.

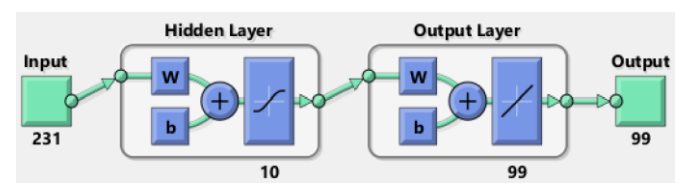


Fig. 6. ANN architecture for IEEE 33 bus distribution system.

4.1.1. Validation of the ANN-based voltage stability assessment

The regression coefficient R is main metric for assessing the relationship of a goal with input values in a given predictive model. A correlation result of 0% means there is no relation at all which implies that results are totally random relative to the targets while a value of 100% defines perfect correlation meaning that results are greatly correlated to the objectives. This metric shows how well the predicted results match the actual values of the goal. 7 demonstrates a bar graph depicting all the R values obtained from the four distinct strategies of training functions with the corresponding evaluation done across a total of nine combinations of activation functions. This form of presentation makes it easy to gauge how well each algorithm performs in comparison to the set tar- gets that were provided. In order of preference, various training functions were tested for the ANN model to establish the best training algorithm for the system under study. This strategy guarantees the best result in both accuracy and generalization, and function se- lection was carried out through comparative evaluation. In the evaluation of all R values, the Levenberg-Marquardt (LM) approach is repeatedly claimed to outdo all competitors in every evaluation. This means that he offers the best and most reliable estimates when made in comparison to all other alternatives available.

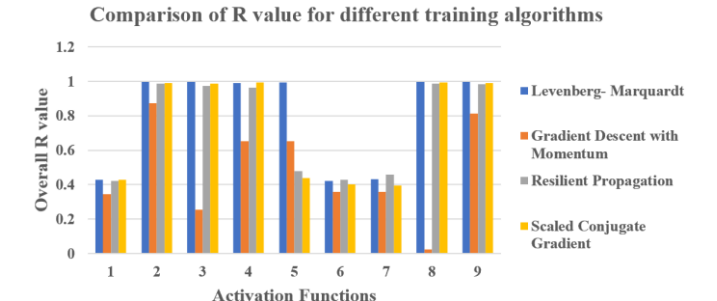


Fig. 7. Comparison of R value for different training algorithms.

Figure 8 illustrates how the mean squared error (MSE) is computed over several training epochs. In table 4, the best prediction accuracy for various training algorithm and activation function combinations is presented. This shows has shown delved into how varying training techniques and activation function settings impact the predictions. The average lowers the MSE, the more effective the model is considered. Performance analysis demonstrates that the Tan-

Lin activation function maintains accuracy and reliability throughout a range of operational training strategies.

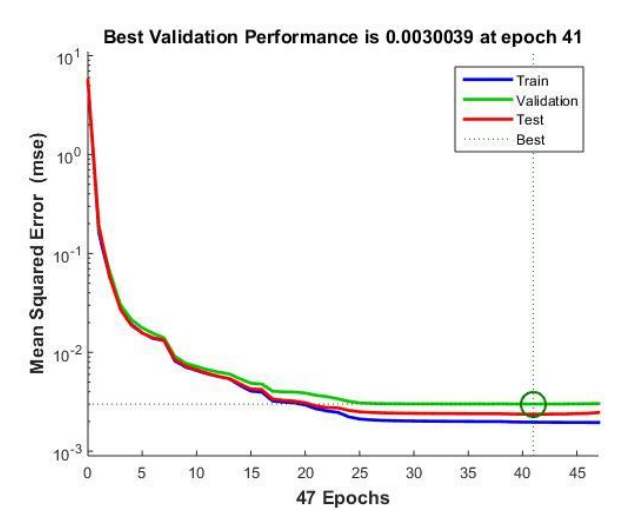


Fig. 8. Variation in mean-squared error of LM algorithm with tan-linear activation.

Table 4. Comparison of regression values (*R*) for different activation function

Activation	Levenberg-	Gradient Descent	Resilient	Scaled Conjugate
functions	Marquardt	with Momentum	Propagation	Gradient
Tan-Log	0.42803	0.34527	0.42132	0.42763
Tan-Lin	0.99649	0.87492	0.98687	0.98964
Log-Tan	0.99613	0.25272	0.97302	0.98777
Log-Lin	0.98973	0.65136	0.96381	0.9939
Lin-Tan	0.99537	0.65291	0.47957	0.43728
Lin-Log	0.42209	0.35641	0.42806	0.40133
Log-Log	0.43175	0.35718	0.45674	0.39465
Lin-Lin	0.99636	0.021886	0.98623	0.99373
Tan-Tan	0.99578	0.81205	0.98281	0.98898

The model improves most between the 60th to 70th epoch, showing nearly 0.0022782 MSE at epoch 65, proving strongest error reduction. R values during advance the summarized obtained during training, validation, testing phases of LM with tan linear activates is demonstrated in figure 9. This figure summarizes the R values obtained during the training, validation, and testing phases of the LM technique with a tan-linear activation function. The results confirm that the LM algorithm is consistent and dependable in its performance, particularly in conjunction with the tan-linear activation function. The illustration proves the reliability and efficiency of the LM algorithm, showcasing its robust performance.

4.2. Analysis of the Results and Discussion

4.2.1. Case-1: SPV penetration at selected busses

SPV systems incur smaller values of VSI on Distribution buses, thus they are integrated into system buses. In order to

illustrate the changes in bus voltages for the various scenarios associated with SPV integration, which include results from Scenarios 2 to 8 as stated in table 3, which is illustrated in figure 10. For a given scenario at a time, all buses voltage magnitudes were captured. The graph indicates that there is an extent to which generation exceeds load demand, which causes the PQ bus to convert to a PV bus, voltage boostering at 1.05 pu and voltage steadiness at the same time and further improving a dependable system with enhanced modular solar power. The generating margin is the region within which additional capacity could be supplied below the limits stated and increase the possibilities without driving these attributes into disruption. In figuring how much solar energy could reasonably be integrated along with adequate control of levels of voltage and limits of passive-active power, this margin becomes interesting. The VSI for 33 buses across 116 scenarios is shown in figure 11. The spikes presented where PQ buses are converted to PV buses show the changes in

operational state of certain buses which are expected to using solar generation on exceed active real power demand.

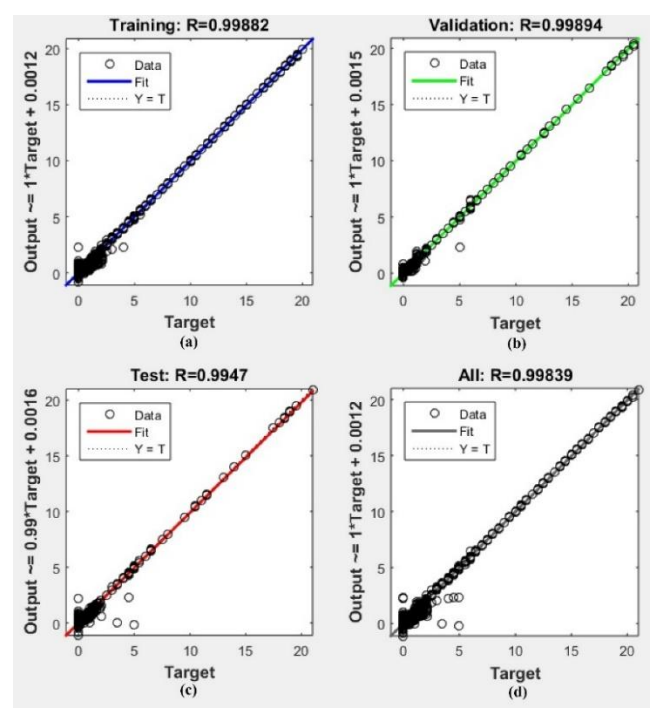


Fig. 9. Variation of regression with the 42 epochs of LM algorithm with tan-linear activation.

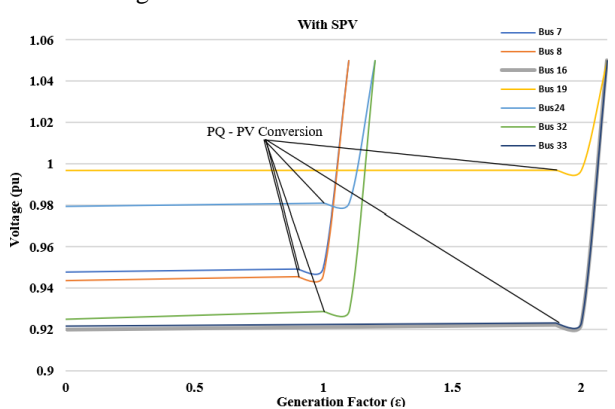


Fig. 10. Variation in bus voltages - case:1.

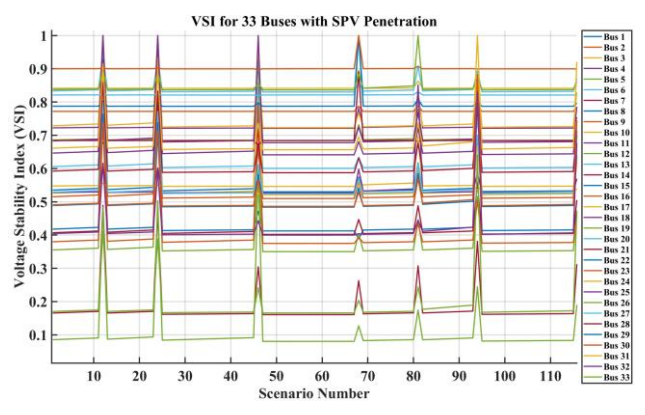


Fig. 11. VSI with different penetration levels of SPV.

4.2.2. Case-2: Penetration of EV charging station at various busses

As seen in table 3, EV charging stations have been integrated into buses with larger VSI in the second scenario. The impact of increasing EV on voltage stability is illustrated in figure 12, which indicates that the voltage in the selected buses diminishes when there is an increase in load demand. Figure 13 illustrates the VSI for 33 busses over 428 scenarios of EV penetration levels. The VSI spike s represent break points when the load demand reaches its maximum limit, which might be critical for the system's voltage stability due to increased demand.

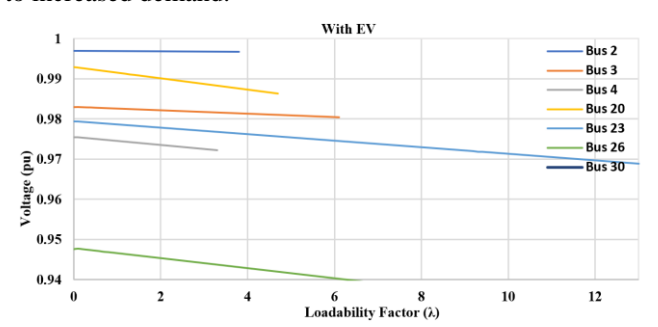


Fig. 12. Variation in bus voltages - case:2.

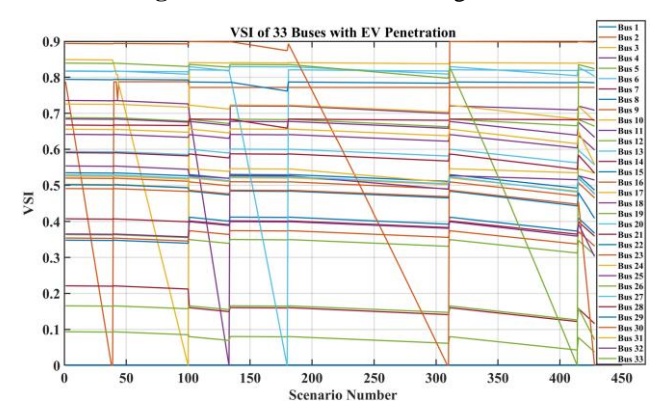


Fig. 13. VSI with different penetration levels of EV charging.

4.2.3. Case-3: Combined penetration of SPV and EV charging stations

Figure 14 demonstrates the voltage behavior of buses under increasing EV and SPV penetration in Case 3 (Table 3). EV-connected buses experience noticeable voltage dips due to charging loads, whereas SPV-connected buses maintain relatively higher voltage levels. The presence of SPV generation helps offset voltage decline typically caused by EV loads. Additionally, converting PQ buses to PV buses (with $\epsilon=1$) results in a sharp voltage rise, further enhancing voltage stability.

Table 3 (entries 16–22) outlines scenarios of simultaneous SPV and EV integration. When penetration levels increase beyond typical operating margins, voltages and VSI values begin to fluctuate, indicating system stress. As shown in Figures 14 and 15, high SPV–EV integration begins to unlock voltage thresholds at the substation level, challenging the system's stability boundaries.

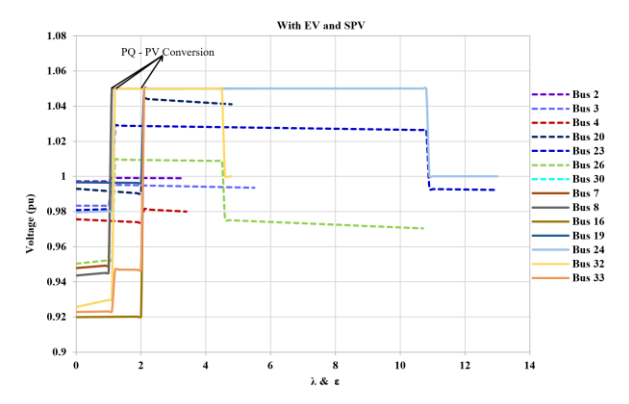


Fig. 14. Variation in bus voltages during SPV and EV penetration - case:3.

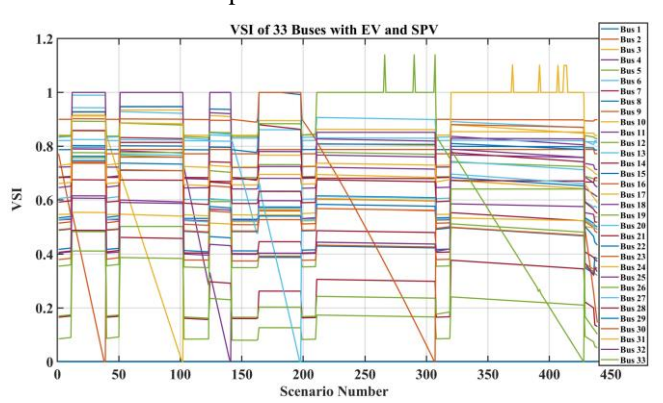


Fig. 15. VSI with SPV and EVs.

In entry 26 of Table 3, a scenario with low SPV (2 units) and high EV (5 units) penetration is analyzed. Figure 16 reveals that this imbalance leads to the steepest voltage drops, particularly at EV-dominant buses. In contrast, SPV buses are less affected. Figure 17 confirms that high EV loading significantly weakens the VSI profile across the network, reinforcing the need for balanced integration of distributed generation and EV demand to preserve system reliability.

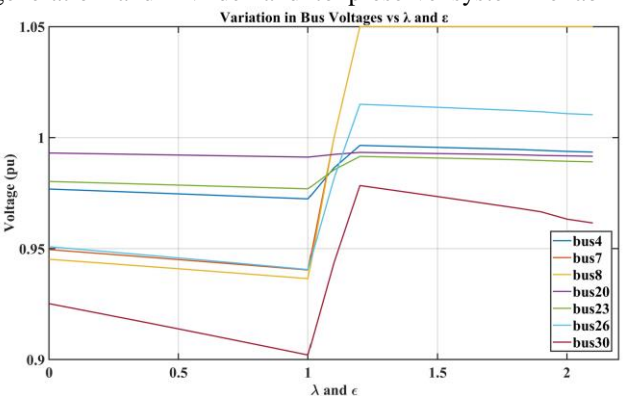


Fig. 16. Variation in bus voltages during high EV penetration and low SPV penetration.

Figure 18 presents the voltage profile for Case 3, Entry 27 (Table 3), involving low EV penetration (2 buses) and high SPV integration (5 buses). In the early stages, voltages rise uniformly across all buses due to high solar power availability. A further boost is observed when PQ buses are converted to PV buses, reinforcing the positive effect of distributed solar generation on system voltage support. Figure 19 shows the corresponding Voltage Stability Index (VSI) across all 33

buses. During peak solar hours, the improved VSI indicates enhanced voltage stability. However, the results also reveal that excessive SPV injection—especially under light loading—may result in overvoltage conditions, signaling a need for coordinated control strategies. These findings highlight that while SPV integration can alleviate voltage drops, unregulated high penetration risks destabilizing the system through voltage exceedance.

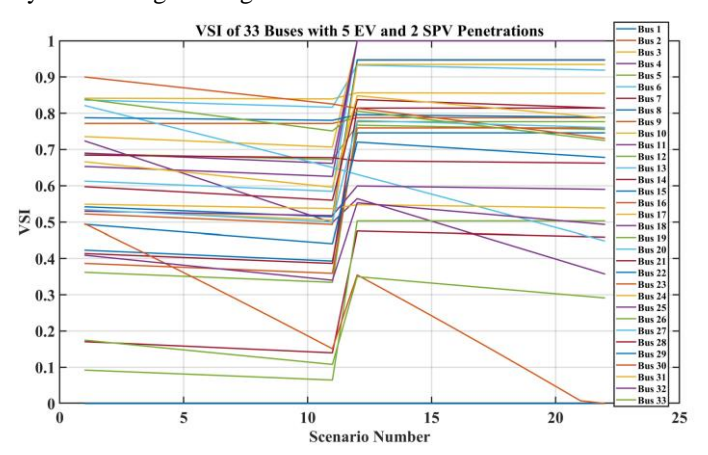


Fig. 17. VSI of 33 buses with high EV penetration and low SPV penetration.

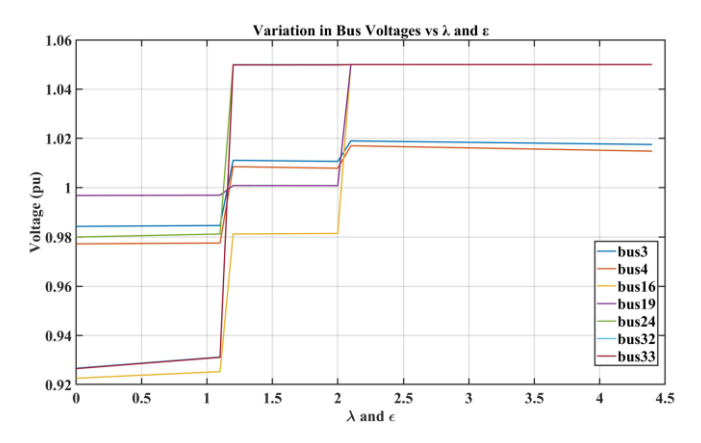


Fig. 18. Variation in bus voltages during high SPV penetration and low EV penetration.

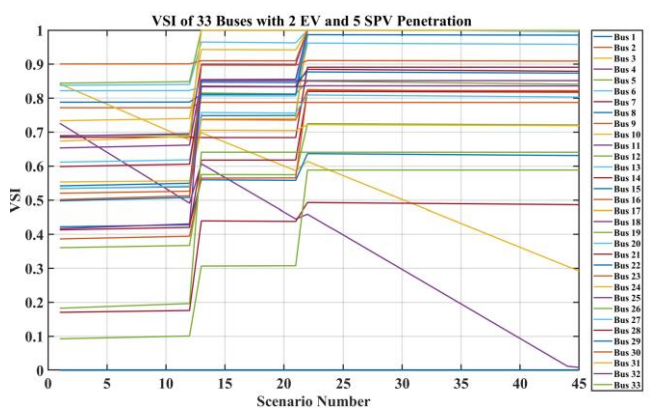


Fig. 19. VSI of 33 buses with high SPV penetration and low EV penetration.

Case 3, Entry 28 (Table 3), illustrated in Figure 20, evaluates system behavior under simultaneous high

penetration of both SPV and EVs (7 buses each). Initially, EV charging demand leads to noticeable voltage dips, but as SPV generation increases, the network voltage recovers due to renewable energy being absorbed by EV loads. However, once SPV generation surpasses consumption, the network again experiences voltage rise beyond nominal levels. Figure 21 reflects this in the VSI trends, showing that while combined SPV–EV integration can stabilize the system under balanced conditions, it can also introduce instability if unmanaged. This complex interaction emphasizes the importance of optimized coordination between renewable generation and flexible demand (e.g., EV charging), supporting the study's insight that intelligent scheduling and real-time voltage regulation.

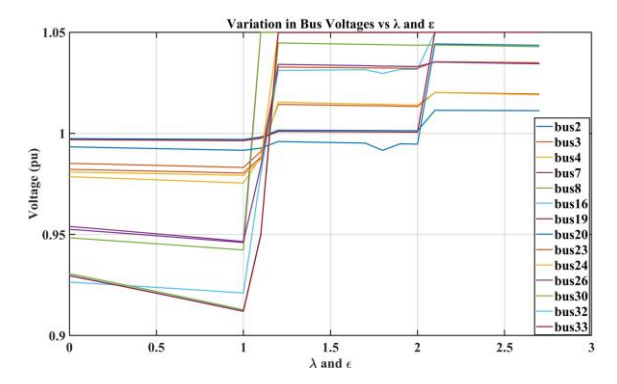


Fig. 20. Variation in bus voltages during higher levels of SPV and EV penetration.

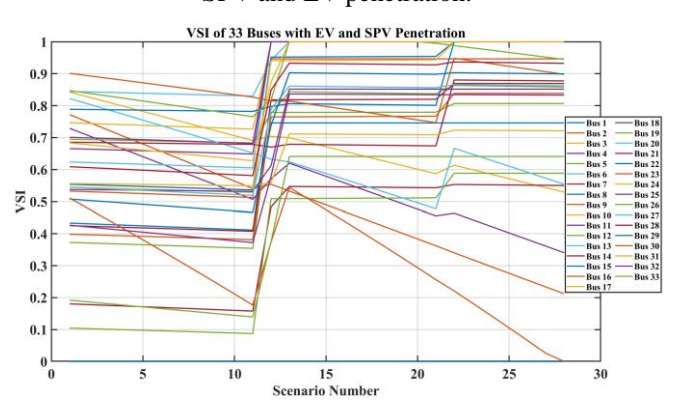


Fig. 21. VSI of 33 buses with higher levels of SPV and EV penetration.

4.3. Predictor-Corrector Continuation Power Flow Results

A continuation power flow method has been used to evaluate the voltage stability characteristics of different distributed energy scenarios. The Predictor-Corrector Continuation Power Flow study was conducted on the IEEE 33-bus radial distribution system in three scenarios: with SPV integration, EV integration, and both SPV and EV integrated. In each case, the 'GAM' and 'LAM' indicators graphs were drawn.

The results from the Predictor-Corrector CPF for the case of SPV-only integration are shown in figure 22. When the generation factor ϵ is increased, voltages at the SPV buses increase slowly at first. If the active power produced at a bus is greater than the local demand $(P_G > P_D)$, that particular bus goes through PQ–PV conversion. This results in a shift of voltage to 1.05 PU. The depicted plot highlights this transition

point. Due to the method's path-following continuation capability, there is efficient capture of the propulsion voltage control mechanism which serves the purpose of strategically routing generation within inert distribution networks.

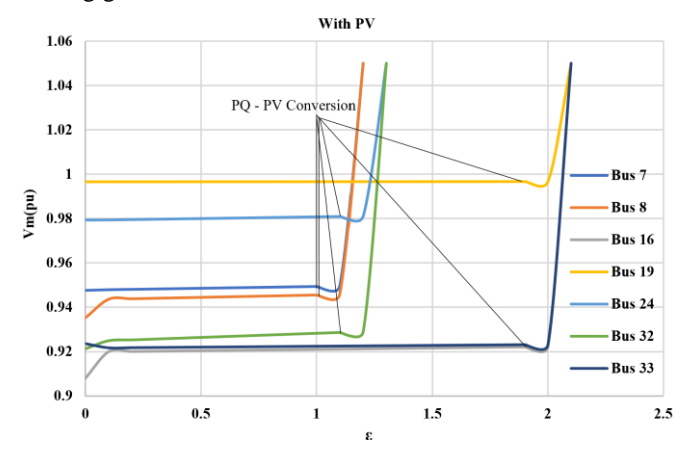


Fig. 22. Variation in bus voltages with SPV Penetration.

Figure 23 shows the CPF results for a scenario with increasing EV loads at Buses 2, 3, 4, 20, 23, 26, and 30, without any local generation. As the loading parameter (λ) increases, these buses experience continuous voltage decline, with no sign of recovery. Remote buses, particularly Bus 30, show early voltage collapse due to their position at the far end of the radial feeder. While this behavior is consistent with expectations in radial networks under high load conditions, CPF effectively tracks the progression of instability, identifying the most vulnerable nodes early in the loadability curve.

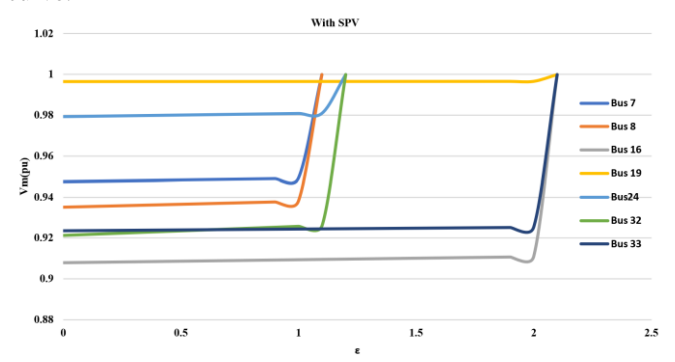


Fig. 23. Variation in bus voltages with EV penetration.

Figure 24 extends this analysis by incorporating simultaneous SPV generation at Buses 7, 8, 16, 19, 24, 32, and 33 alongside the same EV load increase. While the EV-loaded buses still experience voltage reductions, the presence of distributed generation results in improved voltage stability margins and delays the onset of collapse. The key insight here is not just the voltage improvement at SPV buses, but the broader stabilizing effect across the network. This demonstrates that the coordinated deployment of SPV generation near or along stressed feeders can significantly mitigate voltage stress from EV charging loads, offering a practical strategy for enhancing resilience in future distribution systems.

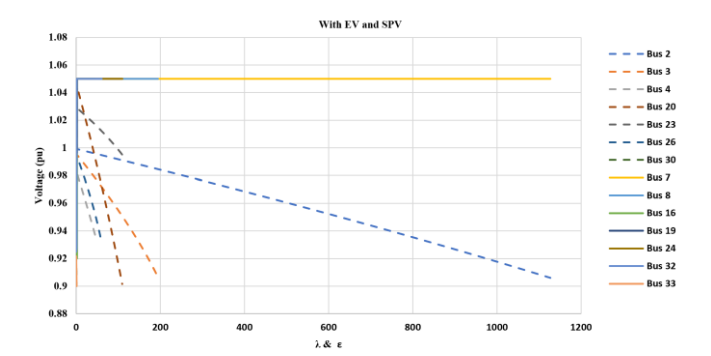


Fig. 24. Variation in bus voltages with SPV and EV penetration.

4.4. Jacobian-Based Sensitivity Analysis Results

In this section, it interpret the results of the Jacobian-Based Sensitivity Analysis (JBSA) applied to the IEEE 33-bus radial distribution system under three operational scenarios: (i) Electric Vehicle (EV) load penetration, (ii) Solar Photovoltaic (SPV) generation integration, and simultaneous SPV and EV presence. Unlike CPF, which maps the full loadability curve, JBSA offers direct insight into how voltage magnitudes respond to incremental power changes through sensitivity factors $\frac{\partial V}{\partial P}$ and $\frac{\partial V}{\partial Q}$, computed using the inverse Jacobian at specific operating points. At the final loadability point $\lambda = 190.6$, corresponding to increased load at Bus 2, the voltage sensitivity factors $\frac{\partial V}{\partial P}$ and $\frac{\partial V}{\partial Q}$ were calculated across all buses. As shown in Figure 25, a sharp peak in both sensitivity metrics is observed near Bus 18. This identifies it as a voltage-sensitive bus, even though the load increase originated from Bus 2. In contrast, Buses 1–5, located close to the substation, display minimal sensitivity. The radial structure of the network inherently causes higher sensitivity in mid and end-feeder buses, reinforcing JBSA's effectiveness in identifying weak nodes prone to voltage collapse.

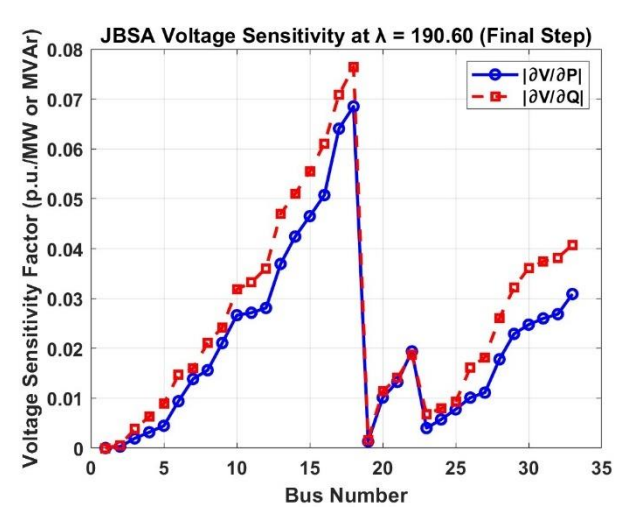


Fig. 25. Voltage sensitivity factors with respect to EV penetration in bus 2.

Under a different condition where generation is increased at Bus 7 up to $\varepsilon=1.20$, the sensitivity profile, shown in Figure 26, still identifies Bus 18 as the most critical point. This result highlights that spatial proximity to the generation

source does not guarantee local voltage stability improvement, especially in radial systems. While SPV injection supports voltage locally, its influence diminishes along the feeder, emphasizing the need for strategic generator placement and coordinated voltage control.

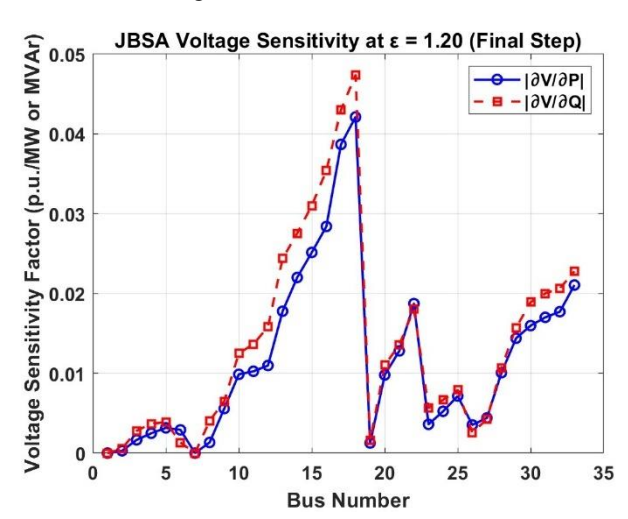


Fig. 26. Voltage sensitivity factors with respect to SPV penetration in bus.

In the third case, simultaneous EV load and SPV generation penetration were modeled with EVs added at Buses 2, 3, 4, 20, 23, 26, and 30, and SPVs at Buses 7, 8, 16, 19, 24, 32, and 33. The resulting sensitivity plot at $\lambda=18.50$ and $\epsilon=2.1$ is depicted in Figure 27. Here, a more distributed sensitivity pattern with multiple peaks is observed. This is indicative of complex interactions between load stress and generation support. Mid and end-feeder buses, once again, show higher sensitivity, underscoring their vulnerability under high EV penetration. Notably, the voltage support from SPV generation appears insufficient to fully mitigate the destabilizing effects of increased EV demand unless coordinated planning is applied.

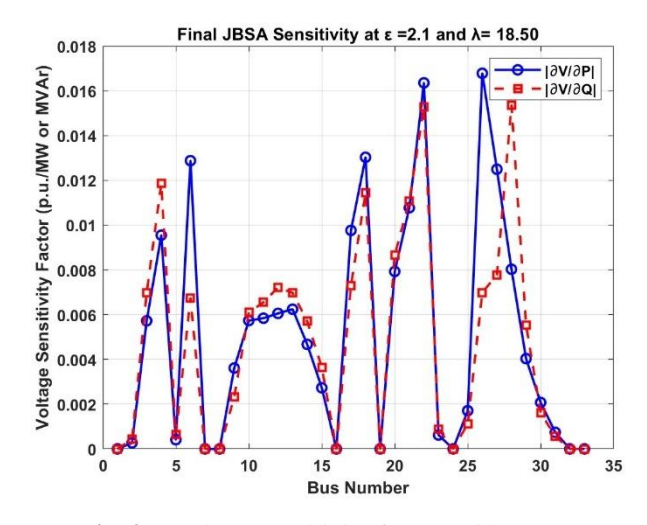


Fig. 27. Voltage sensitivity factors with respect to simultaneous SPV and EV penetration.

4.5. Comparison of Voltage Stability Analysis Methods

The IEEE 33-bus radial distribution system is analyzed in terms of memory and computational time against varying stability assessment using three methodologies—Predictor-Corrector Continuation Power Flow (CPF), Jacobian-Based Sensitivity Analysis (JBSA), and Artificial Neural Network (ANN) is illustrated in table 5. Although CPF was accurate and traced the entire loadability path, it took the longest time

of 20.34 minutes and moderate memory of 7.64 MB. JBSA spent only 2.86 minutes due to significant computation time savings, but used more memory (21.90 MB) because of the necessity to retain the complete Jacobian matrix and the approach, how- ever, completed the assessment in 0.6 seconds while using the least amount of memory (3.0265 MB), which increases the appeal of the method for real-time applications and quick decision making.

Table 5. Comparison of voltage stability analysis methods

Voltage Stability Analysis Methods	Memory Required (MB)	Total Time Required
CPF	7.64	20.34 minutes
JBSA	21.90	2.86 minutes
ANN	3.0265	0.6 seconds

5. Conclusion

In this paper, it developed a complete framework for voltage stability analysis of radial distribution systems with high penetrations of Electric Vehicles (EVs) and Solar Photovoltaics (SPVs) using three approaches: Predictor-Corrector Continuation Power Flow (CPF), Jacobian-Based Sensitivity Analysis (JBSA), and a proposed Artificial Neural Network (ANN) model. The developed ANN model was trained on detailed datasets developed for different operational scenarios such as simultaneous EV load increases and SPV generation at fundamental buses of the IEEE 33-bus radial distribution system.

The CPF method precisely traces the P–V curves, as well as the loadability limits and point of voltage collapse. It estimates crucial indicators like Loadability Margin (LAM) and Generation Admissibility Margin (GAM) which supports effective understanding of system stability. However, due to the computational and time-intensive nature of the process, CPF is not real-time suitable. JBSA, on the other hand, analyzes the Jacobian matrix to provide a rapid assessment of voltage sensitivity factors which is very useful in terms of localizing weak buses. Although this method is faster than CPF, its high memory consumption without real-time responsiveness is still a disadvantage.

The limitations described earlier are solved with the incorporation of VSI, LAM, and GAM as features and indicators at the system level in the proposed ANN-based method, which enables accurate and instantaneous stability predictions. The predictive accuracy achieved by the model using ANN is remarkable, considering it takes only 0.6 seconds and 3.0265 MB of memory, compared to the CPF's 20.34 minutes and 7.64 MB, and JBSA's 2.86 minutes and 21.90 MB, both significantly higher in taxpayer resources in comparison to the ANN model. Moreover, the model's adaptability under changing operational conditions enhances its reliability in real-time stability monitoring.

In conclusion, the combination of LAM, GAM, VSI, and ANN boosts the voltage stability assessment associated with modern distribution systems. The findings validate the

practicality of the proposed ANN model as it offers a dependable solution that is easily scaled and computed against the conventional techniques of CPF and JBSA, in particular for application in smart grids with high decentralized energy resources and electric vehicle integration due to the speed sensitivity of the system. Incorporating real- time forecasting of SPV generation and stochastic modeling of EV charging behaviors will be elements to consider in further work, along with optimization-based placement strategies for distributed generation and storage units.

References

- [1] R. Wang, X. Bi, S. Bu, "Real-time coordination of dynamic network reconfiguration and volt-var control in active distribution network: A graph-aware deep reinforce- ment learning approach," IEEE Trans. Smart Grid, vol. 15, no. 3, pp. 3288–3302, 2024. doi:10.1109/TSG.2023.3324474.
- [2] L. Peng, A. Zabihi, M. Azimian, H. Shirvani, and F. Shahnia, "Developing a robust expansion planning approach for transmission networks and privately-owned renewable sources," IEEE Access, vol. 11, pp. 76046–76058, 2023, doi: 10.1109/ACCESS.2022.3226695.
- [3] W. Huang, W. Zheng, D. J. Hill, "Distribution network reconfiguration for short-term voltage stability enhancement: An efficient deep learning approach," IEEE Trans. Smart Grid, vol. 12, no. 6, pp. 5385–5395, 2021. doi:10.1109/TSG.2021.3097330.
- [4] R. Yan, T. K. Saha, "Investigation of voltage stability for residential customers due to high photovoltaic penetrations," IEEE Trans. Power Syst., vol. 27, no. 2, pp. 651–662, 2012. doi:10.1109/TPWRS.2011.2180741.
- [5] S. Nandi, S. R. Ghatak, P. Acharjee, "Placement of EV fast charging station in distribution system based on voltage stability index strategy," in Proc. 6th IEEE Int. Conf. Condition Assessment Techniques in Electrical Systems (CATCON), 2022, pp. 46–51. doi:10.1109/CATCON56237.2022.10077648.

- [6] A. Tavakoli, S. Saha, M. T. Arif, M. E. Haque, N. Mendis, A. M. T. Oo, "Impacts of grid integration of solar PV and electric vehicle on grid stability, power quality and energy economics: A review," IET Energy Syst. Integr., vol. 2, no. 3, pp. 243–260, 2020. doi:10.1049/iet-esi.2019.0047.
- [7] N. K. K., J. N. S., V. K. Jadoun, "A combined approach to evaluate power quality and grid dependency by solar photovoltaic based EV charging station using hybrid optimization," J. Energy Storage, vol. 84, 110967, 2024. doi:10.1016/j.est.2024.110967.
- [8] N. Sanampudi, P. Kanakasabapathy, "Integrated voltage control and frequency regulation for stand-alone microhydro power plant," Materials Today: Proc., vol. 46, pp. 5027–5031, 2021. doi:10.1016/j.matpr.2020.10.403.
- [9] M. M. Haque, P. Wolfs, "A review of high PV penetrations in LV distribution net- works: Present status, impacts and mitigation measures," Renew. Sustain. Energy Rev., vol. 62, pp. 1195–1208, 2016. doi:10.1016/j.rser.2016.04.025.
- [10] M. Karimi, H. Mokhlis, K. Naidu, S. Uddin, A. H. A. Bakar, "Photovoltaic penetration issues and impacts in distribution network—A review," Renew. Sustain. Energy Rev., vol. 53, pp. 594–605, 2016. doi:10.1016/j.rser.2015.08.042.
- [11] J. Suganya, R. Karthikeyan, J. Ramprabhakar, "Voltage stabilization by using buck converters in the integration of renewable energy into the grid," in New Trends in Computational Vision and Bio-Inspired Computing. Springer, 2020, pp. 103–113. doi:10.1007/978-3-030-41860-0 10.
- [12] K. R. Bharath, H. Choutapalli, P. Kanakasabapathy, "Control of bidirectional DC— DC converter in renewable-based DC microgrid with improved voltage stability," International Journal of Renewable Energy Research, vol. 8, no. 2, p. 7509, 2018.
- [13] A. Zabihi and M. Parhamfar, "EMPOWERING THE GRID: Toward the integration of electric vehicles and renewable energy in power systems," International Journal of Energy Security and Sustainable Energy (IJESSE), vol. 2, no. 1, pp. 1–14, Jul. 2024, doi: 10.5281/zenodo.12751722.
- [14] R. Gadal, O. Aziz, F. Elmariami, A. Belfqih, N. Agouzoul, "Voltage stability assessment and control using indices and FACTS: A comparative review," J. Electr. Comput. Eng., 2023, Art. ID 5419372. doi:10.1155/2023/5419372.
- [15] H. S. Salama, I. Vokony, "Voltage stability indicesa comparison and a review," Comput. Electr. Eng., vol. 98, 107743, 2022. doi:10.1016/j.compeleceng.2022.107743.
- [16] A. Selim, S. Kamel, A. S. Alghamdi, F. Jurado, "Optimal placement of DGs in distribution system using an improved Harris Hawks optimizer based on single- and multi-objective approaches," IEEE Access, vol. 8, pp.

- 52815–52829, 2020. doi:10.1109/ACCESS.2020.2980245.
- [17] A. A. Mohamed Faizal, N. Dwivedi, M. Sivasubramanian, S. Marisargunam, K. Rajesh, and N. Janaki, "Voltage stability improvement using PV coordinated control scheme in IEEE-9 bus system," in Proc. ICRP, 2023, Springer, 2024.
- [18] A. A. Mohamed Faizal, N. Dwivedi, M. Sivasubramanian, S. Marisargunam, K. Rajesh, and N. Janaki, "A combined approach to evaluate power quality and grid dependency by solar photovoltaic based electric vehicle charging station using hybrid optimization," J. Energy Storage, 2024.
- [19] K. Anthony and V. Arunachalam, "Voltage stability monitoring and improvement in a renewable energy dominated deregulated power system: A review," e-Prime Adv. Electr. Eng., Electron. Energy, vol. 11, 2025, Art. no. 100893, doi: 10.1016/j.prime.2024.100893.
- [20] S. Ly, A. Singh, P. Vorobev, Y. C. Soh, and H. D. Nguyen, "Chance-constrained solar PV hosting capacity assessment for distribution grids using Gaussian Process and Logit learning," arXiv preprint, arXiv:2505.19839, 2025.
- [21] PV magazine International, "EV charging shapes PV investment, grid load in community study," pv magazine International, Jun. 12, 2025. [Online]. Available: https://www.pv-magazine.com/2025/06/12/ev-charging-shapes-pv-investment-grid-load-in-community-study/
- [22] K. D. Dharmapala, A. Rajapakse, K. Narendra, Y. Zhang, "Machine learn- ing based real-time monitoring of long-term voltage stability using volt- age stability indices," IEEE Access, vol. 8, pp. 222544–222555, 2020. doi:10.1109/ACCESS.2020.3043935.
- [23] H. H. Goh, Q. S. Chua, S. W. Lee, B. C. Kok, K. C. Goh, K. T. K. Teo, "Evaluation of voltage stability indices in power systems using an artificial neural network," Procedia Eng., vol. 118, pp. 1127–1136, 2015. doi:10.1016/j.proeng.2015.08.454.
- [24] A. K. Sharma, A. Saxena, B. P. Soni, V. Gupta, "Voltage stability assessment using artificial neural network," in IEEE Int. Conf. Electrical, Computer and Communication Technologies (ICECCT), 2018, pp. 1–6. doi:10.1109/ICECCT.2018.8475510.
- [25] S. Sathyan, V. Pandi, A. Antony, S. R. Salkuti, P. Sreekumar, "ANN-based energy management system for PV-powered EV charging station with battery backup and vehicle-to-grid support," Int. J. Green Energy, vol. 21, pp. 1–16, 2023. doi:10.1080/15435075.2023.2246048.
- [26] R. D. Zimmerman, C. E. Murillo-Sa'nchez, R. J. Thomas, "MATPOWER: Steady-state operations, planning, and analysis tools for power systems research and education," IEEE Trans. Power Syst., vol. 26, no. 1, pp. 12–19, 2011. doi:10.1109/TPWRS.2010.2051168.

- [27] R. D. Zimmerman, C. E. Murillo-Sa'nchez, MATPOWER User's Manual, Ver. 7.1.2020. doi:10.5281/zenodo.4074122.
- [28] B. Bakhshideh Zad, J. Lobry, F. Valle'e, "A new voltage sensitivity analysis method for medium-voltage distribution systems incorporating power losses impact," Electr. Power Components Syst., vol. 46, nos. 14–15, pp. 1540–1553, 2018. doi:10.1080/15325008.2018.1511639.
- [29] M. Tostado, S. Kamel, F. Jurado, "Developed Newton–Raphson based predic-tor–corrector load-flow approach with high convergence rate," Int. J. Electr. Power Energy Syst., vol. 105, pp. 785–792, 2019. doi:10.1016/j.ijepes.2018.09.021.
- [30] N. Hatziargyriou, J. Milanoviç, C. Rahmann, V. Ajjarapu, C. Canizares, I. Erlich, "Definition and classification of power system stability-revisited & extended," IEEE Trans. Power Syst., vol. 36, no. 4, pp. 3271–3281, 2021. doi:10.1109/TPWRS.2020.3041774.
- [31] K. Suresh, P. Kanakasabapathy, "A review of voltage stability issues in distribution system influenced by high PV penetration and its mitigation techniques," Int. J. Renew. Energy Res., vol. 13, no. 1, pp. 236–244, 2023. doi:10.20508/ijrer.v13i1.13388.g8678.
- [32] J. Modarresi, E. Gholipour, A. Khodabakhshian, "A comprehensive review of the voltage stability indices," Renew. Sustain. Energy Rev., vol. 63, pp. 1–12, 2016. doi:10.1016/j.rser.2016.05.010.
- [33] S. Mokred, Y. Wang, "Voltage stability assessment and contingency ranking in power systems based on a modern stability assessment index," Results Eng., vol. 23, 102548, 2024. doi:10.1016/j.rineng.2024.102548.
- [34] M. Aldeen, S. Saha, T. Alpcan, "Voltage stability margins and risk assessment in smart power grids," IFAC Proc. Vol., vol. 47, no. 3, pp. 8188–8195, 2014. doi:10.3182/20140824-6-ZA-1003.02102.
- [35] S. Mokred, Y. Wang, T. Chen, "Modern voltage stability index for prediction of volt- age collapse and estimation of maximum load-ability," Int. J. Electr. Power Energy Syst., vol. 145, 108596, 2023. doi:10.1016/j.ijepes.2022.108596.

- [36] S. Mokred, Y. Wang, T. Chen, "A novel collapse prediction index for voltage stability analysis and contingency ranking in power systems," Prot. Control Mod. Power Syst., vol. 8, no. 1, pp. 1–27, 2023. doi:10.1186/s41601-023-00279-w.
- [37] J. P. Roselyn, D. Devaraj, S. S. Dash, "Multi-objective genetic algorithm for voltage stability enhancement using rescheduling and FACTS devices," Ain Shams Eng. J., vol. 5, no. 3, pp. 789–801, 2014. doi:10.1016/j.asej.2014.04.004.
- [38] A. N. Archana, T. Rajeev, "A novel reliability index based approach for EV charging station allocation in distribution system," IEEE Trans. Ind. Appl., vol. 57, no. 6, pp. 6385–6394, 2021. doi:10.1109/TIA.2021.3109570.
- [39] M. I. Akbar, S.A.A. Kazmi, O. Alrumayh, Z. A. Khan, A. Altamimi, M. M. Malik, "A novel hybrid optimization-based algorithm for optimal DG allocations in distribution networks," IEEE Access, vol. 10, pp. 25669–25687, 2022. doi:10.1109/ACCESS.2022.3155484.
- [40] T. H. B. Huy, D. N. Vo, K. H. Truong, T. Van Tran, "Optimal distributed generation placement in radial distribution networks using enhanced search group algorithm," IEEE Access, vol. 11, pp. 103288–103305, 2023. doi:10.1109/ACCESS.2023.3316725.
- [41] A. K. Barnwal, L. K. Yadav, M. K. Verma, "A multiobjective approach for voltage stability enhancement and loss reduction via reconfiguration and DG allocation," IEEE Access, vol. 10, pp. 16609–16623, 2022. doi:10.1109/ACCESS.2022.3146333.
- [42] A. M. Tahboub, V. R. Pandi, H. H. Zeineldin, "Distribution system reconfigu- ration for annual energy loss reduction considering variable distributed generation profiles," IEEE Trans. Power Delivery, vol. 30, no. 4, pp. 1677–1685, 2015. doi:10.1109/TPWRD.2015.2424916.
- [43] S. H. Dolatabadi, M. Ghorbanian, P. Siano, N. D. Hatziargyriou, "An enhanced IEEE 33-bus benchmark test system for distribution system studies," IEEE Trans. Power Syst., vol. 36, no. 3, pp. 2565–2572, 2021. doi:10.1109/TPWRS.2020.3038030.